

LETTER

Destruction behavior in high voltage diode with the field limiting ring termination

Lei Zhang¹, Cailin Wang^{1a)}, and Yang Song¹

Abstract The turn-off of high voltage diode under over-stress condition may lead to the diode destruction, which appears at the edge of termination or in the active region. The diode destruction behaviors related to current filament, electric field and maximum temperature are investigated by electrothermal simulation. The results show that the electric field punch-through to the termination surface is unavoidable. The disappearance of current filament at the edge of termination should be a self-stabilizing mechanism because of the extraction of carriers. The reasons for leading to the diode destruction at the edge of termination or in the active region are found.

Keywords: dynamic avalanche, current filament, high voltage diode, reverse recovery

Classification: Power devices and circuits

1. Introduction

Great challenge for the high voltage diode in the IGBT application is to ensure fast and soft recovery behavior [1]. When the high voltage diode is turned off with very high di/dt , high parasitic inductance L and high supply voltage V_{dc} , the dynamic avalanche will occur [2, 3, 4]. The strong current filaments induced by dynamic avalanche lead to the diode destruction [5, 6, 7], and the destruction positions may appear at the edge of the termination or in the active region [8, 9]. Fig. 1 shows the measured failure $I-V$ characteristic of a 6.5 kV diode beyond the safe operating region (SOA) during reverse recovery. The junction termination can improve significantly the robustness of reverse breakdown in high voltage diode. The field limiting ring (FLR) termination is widely used because of its simplicity of the process [10, 11, 12, 13]. During reverse recovery in high voltage diode, the current filament occurs at the edge of the termination due to extracted holes from the n^- base region under reverse applied voltage [14, 15, 16]. This may lead to the diode destruction by local heating. In addition, for the planar termination structure, at the edge of the termination, extracted holes can compensate a part of the acceptor doping and the electric field may punch through to the termination surface or a position close to the surface, giving rise to the diode destruction [14, 17]. Therefore, it is very important to study the current filament in the FLR diode and further reveal the destruction mechanism of the diode.

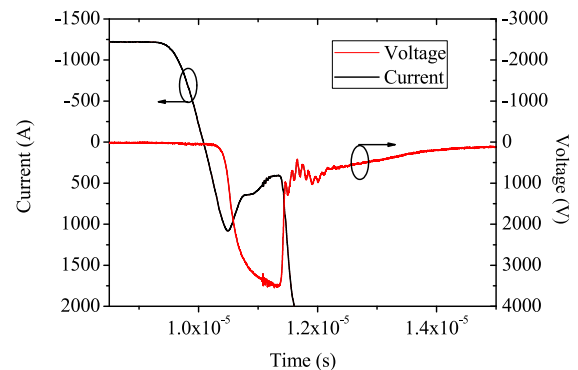


Fig. 1. Measured failure $I-V$ characteristic of a 6.5 kV diode during reverse recovery ($I_F = 2 \times I_{rated} = 1200$ A, $V_{dc} = 4400$ V).

Even through experimental verification, it is still difficult to intuitively get the initial location of the device destruction and to indirectly get a conclusion about the destruction type [18, 19]. Electrothermal simulation of the device is a very useful tool to understand and predict the failure mechanism of the diode during reverse recovery [20, 21]. In this paper, we investigate the destruction behaviors under over-stress condition in the FLR diode by electrothermal simulation, and analyze the reasons for leading to the diode destruction.

2. Device structure and simulation models

We considered the $p^+n^-nn^+$ structure diode with a blocking capability of 3.3 kV, as shown in Fig. 2. The surface doping concentrations of p^+ and n^+ emitters are $1.0 \times 10^{19} \text{ cm}^{-3}$ and $1.0 \times 10^{20} \text{ cm}^{-3}$, and the depths are 30 μm and 10 μm , respectively. The n^- base doping is $N_D = 2.3 \times 10^{13} \text{ cm}^{-3}$. The simulated active region width and thickness of the diode model are 2000 μm and 360 μm , respectively.

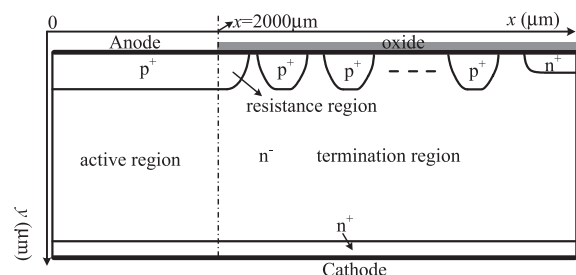


Fig. 2. Schematic view of the diode with the FLR termination structure.

¹Department of Electronic Engineering, Xi'an University of Technology, Xi'an 710048, China

a) wangcailin65@126.com

DOI: 10.1587/elex.16.20190076
Received February 6, 2019
Accepted March 26, 2019
Publicized April 8, 2019
Copyedited April 25, 2019

The n^+ doping stop ring is set at the edge of the device to improve the stability of reverse breakdown voltage. For the FLR structure, the proper ring width, ring spacing and ring number in the termination region are chosen to achieve a maximum breakdown voltage of 3660 V, and the width of the termination region is $\approx 1400 \mu\text{m}$. The resistance region of $100 \mu\text{m}$ width in the diode is designed to relieve the current filament at the end of the active region, and improve the ruggedness of the diode.

The diode was simulated with an extreme over-stress condition, in which $V_{dc} = 2.3 \text{ kV}$, $J_F = 300 \text{ A/cm}^2$, $L = 0.25 \mu\text{H}$ and $di/dt = 9.2 \text{ kA}/\mu\text{s}$, and was analyzed under electrothermal simulation by the Sentaurus-TCAD software. A thermal resistance of 0.1 K/W was set at the cathode-side with an initial temperature $T = 300 \text{ K}$. We considered the Auger and Shockley–Read–Hall recombination models, carrier–carrier scattering, doping dependent and electric field dependent mobility models, and avalanche generation model [22]. The homogeneous carrier lifetimes in the diode are $\tau_p = 0.4 \mu\text{s}$ and $\tau_n = 1.6 \mu\text{s}$.

3. Electric field punch-through induced holes

During reverse recovery, the holes move towards the anode-side in the n^- base, and the electrons move towards the cathode-side. At the p^+n^- junction, the holes and the ionized donors of n^- base region have the same positively charge, hence the effective doping in n^- base region is

$$N_{\text{eff}} = N_D + p \quad (1)$$

where N_D is the doping concentration of ionized donors in n^- base region, p is the on-state hole density. Therefore the electric field gradient in n^- base region can be given by

$$\frac{dE}{dy} = \frac{q(N_D + p)}{\epsilon} \quad (2)$$

With the increase of the reverse current density, dE/dy increases, leading to the steeper dE/dy . The dynamic avalanche occurs at a voltage far below the static breakdown voltage V_{BD} during the diode turn-off [17, 23].

During reverse recovery, the avalanche generated holes and the on-state holes move towards the anode-side. Similar to the peak electric field shifting of p^+n^- junction induced by avalanche generated carriers after the onset of static avalanche [24], the peak electric field shifting also occurs at the p^+n^- junction under dynamic avalanche. According to the Poisson equation, the electric field gradient (dE'/dy) after shifting in the p^+ region is given by,

$$\frac{dE'}{dy} = \frac{q(p + p_{av} - N_a - n_{av})}{\epsilon} \quad (3)$$

where N_a is the doping concentration of ionized acceptors in the p^+ region. If $p + p_{av} > N_a + n_{av}$, the peak electric field at the pn^- junction shifts to the p^+ region [24]. With the increases of the on-state holes p and the avalanche generated holes p_{av} , they overcompensate the ionized acceptors N_a and the avalanche generated electrons n_{av} , leading to the peak electric field shifting. It means that the peak electric field punches through to the termination surface or a position close to the surface [14].

4. Results and analyses

4.1 Current filament behaviors under over-stress condition

Fig. 3 shows the simulated reverse recovery characteristic of the diode. With the extraction of the plasma in n^- base region, the dynamic avalanche occurs, leading to the appearance of the negative differential resistance [25, 26]. Therefore the reverse voltage rises slowly in the initial stage of the establishment of space charge region. Under such extreme commutation condition, the diode shows the behavior of switching self clamping mode (SSCM) [27] during reverse recovery.

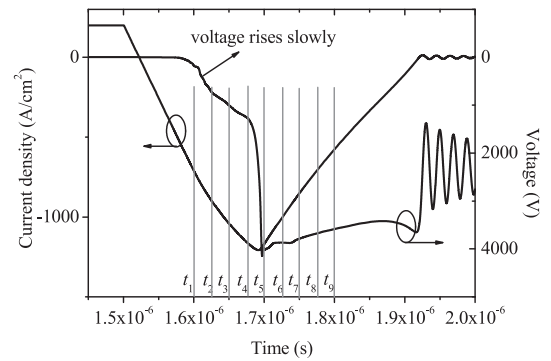


Fig. 3. Simulated reverse recovery characteristic of the diode.

In order to investigate the behavior of current filaments, Fig. 4 shows the evolution of current density distributions of three dimension (3D) in the diode at different times during reverse recovery. During $t_1 \sim t_9$, the evolution process of current filaments in the diode can be roughly divided into three phases:

Phase 1 ($t_1 \sim t_3$): The current filament rises at the edge of the termination. The on-state holes of the termination have to be extracted by reverse applied voltage during reverse recovery, flowing through the edge of the termination. This leads to very high current density here, and triggering the first current filament, as shown at $t_1 = 1.60 \mu\text{s}$. With the increase of hole density, the current filament gradually rises to its maximum value at $t_3 = 1.65 \mu\text{s}$ in the diode.

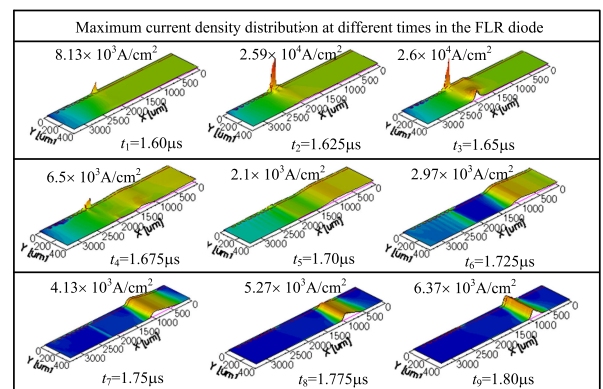


Fig. 4. Evolution of current density distributions of three dimension (3D) in the diode at different times during reverse recovery ($x = 0 \sim 2000 \mu\text{m}$: active region, $x = 2000 \sim 3400 \mu\text{m}$: termination region, $y = 0 \mu\text{m}$: anode, $y = 360 \mu\text{m}$: cathode).

Phase 2 ($t_3 \sim t_5$): The current filament at the edge of the termination decreases and transfers to the active region. With the extraction of carriers, the space charge region extends quickly towards the end of the termination, and the termination region begins to undertake the voltage across the diode, leading to the decrease of the plasma. As a results, the current filament at the edge of the termination decreases and transfers to the active region. At $t_5 = 1.70 \mu\text{s}$, the current filament in the active region dominates, and the plasma layer has disappeared at this moment. The total current density is undertook by the current filament extending from the anode-side to the cathode-side.

Phase 3 ($t_5 \sim t_9$): The current filament rises in the active region. At $t_6 = 1.725 \mu\text{s}$, the single current filament connected to the anode-side and the cathode-side remains in the diode. The filament is maintained by the positive feedback between two carrier-generating high-field regions located in the anode-side and the cathode-side depletion layers, respectively [25]. The width of filament reduces, due to the extraction of residual carriers in the n^- base and the avalanche generated carriers tending to move towards the center of filament where the resistivity is minimum. These provoke the rise of current filament in the active region.

4.2 Destruction mechanism

Fig. 5 indicates electric field strength distributions of the diode under reverse breakdown and during reverse recovery. From the left of Fig. 5, the peak electric field is inside the body of the device under reverse breakdown. During reverse recovery, the current filament at the edge of the termination can reach the maximum value due to the extraction of holes, and almost at the same time, the electric field strength inside the filament also reaches the peak value at $t = 1.665 \mu\text{s}$, as shown in the middle of Fig. 5. It can be observed that the peak electric field punches through to the termination surface at $t = 1.665 \mu\text{s}$. In the FLR diode, this phenomenon becomes unavoidable, because the space charge region is not yet fully established in the termination region at the initial stage of reverse recovery. In addition, $(p + p_{av})$ are so higher that they overcompensate the lightly doped N_a at the end of the p resistance region according to Eq. (3), leading to the peak electric field shifting in the p region. Therefore the electric field of punch-through leads to the enhanced impact ionization and provokes more avalanche generated carriers at the termination surface, where the high current filament always flows through. However, after the current filament of the active region dominating, the peak electric field has to transfer into the active region, as shown at the right of Fig. 5. It shows that a strong Egawa field [28] occurs inside the single current filament.

Maximal temperature occurring at a local position during reverse recovery of the diode is shown in Fig. 6. It shows that, the temperature first rises to the peak value with the time (349 K at $t = 1.695 \mu\text{s}$), then falls to a lower value, and finally continues its increase to the maximal value (450 K). Actually, the variation curve of temperature in Fig. 6 is related to the evolution process of current filament of Fig. 4.

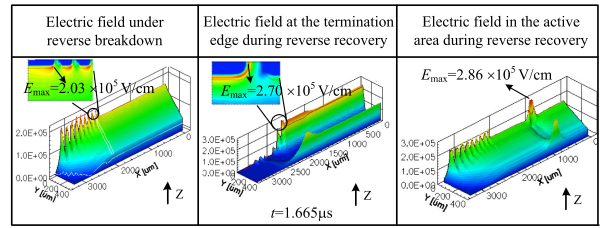


Fig. 5. Electric field strength distributions of three dimension (3D) of the diode. Inset: local electric field strength distributions in two dimension (2D) (Z direction: electric field strength).

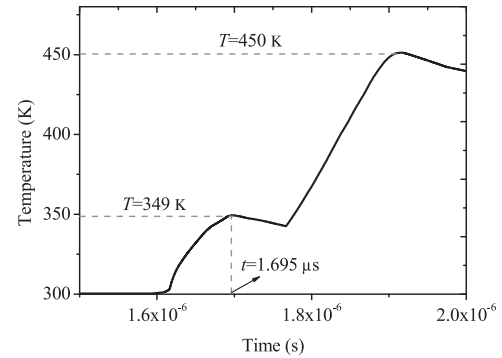


Fig. 6. Maximal temperature occurring at a local position during reverse recovery.

In the phase 1, the temperature increases with the rise of current filament, and then it reaches the maximal temperature (349 K) at the edge of the termination after the current filament reaching a maximum, as shown at the left of Fig. 7, which corresponds to the first temperature peak of Fig. 6 occurring at $t = 1.695 \mu\text{s}$. At the left of Fig. 7, it should be mentioned that the maximal temperature occurs at the position of the peak electric field (the middle of Fig. 5), i.e. at the centre of the carrier-generating located in high-field region. Like high electric field, high impact ionization and high current filament, such these physical effects influence mutually by themselves and maintain a positive feedback process at the termination surface. As a result, the temperature of the termination surface rises its maximum (349 K). In the phase 2, the temperature falls in a short time with the decrease of current filament at the edge of the termination, as shown in Fig. 6. In the phase 3, the temperature gradually rises to its maximum (450 K) with the rise of the single current filament in the active region, as shown at the right of Fig. 7.

Based on the above discussions, we can drawn the following conclusions:

- During reverse recovery, the current filament first appears at the edge of the termination due to the extraction of holes. Although a heavily doped resistance region is designed at the end of the active region to inhibit the current filament and to reduce the failure rate [14], the phenomenon that the high electric field punches through to the termination surface is unavoidable. This triggers the stronger dynamic avalanche, and a local heating occurs at the center of the carrier-generating located in high-field region, leading to an increase of the temperature there. In

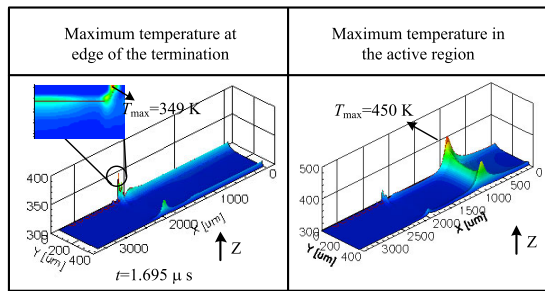


Fig. 7. Maximal temperature distributions of three dimension (3D) at different times during reverse recovery. Inset: local temperature distribution in two dimension (2D) (Z direction: temperature).

real device, the edge of the termination region is very strong inhomogeneity, and it is easier to trigger the first filament [20, 29]. These may be the reasons that lead to the diode destruction at the edge of the termination.

- With the extraction of the plasma layer, the holes can not maintain the high current filament at the edge of the termination, then the current filament begins to drop to a low value, and meanwhile, the current filament arises in the active region. This leads to a short decrease of the maximum temperature inside the diode, which should be a self-stabilizing mechanism. Experiment has been shown that a well-designed and sufficiently robust termination can withstand the high current filament, avoiding the diode destruction at the edge of the termination [30].

- The current filament rises in the active region, and filament extends from the anode-side to the cathode-side after the disappearance of the plasma layer. When it dominates in the active region, the single current filament carries the total current across the whole diode, and transforms into the filament essentially driven by thermal mechanism [25], leading to the increase of the temperature at the anode-side, as shown at the right of Fig. 7. This may lead to the diode destruction in the active region. It is assumed that the aluminum wire is firm at the surface of the active region. The high temperature near the p^+n^- junction at the anode-side may give rise to the melting by local heating below the wafer surface [9]. In the fact, whereas, the current filament is a three dimension (3D) effect which likes a column, and this leads to the higher temperature than that of two dimension (2D) simulation [17].

5. Conclusion

We investigated the destruction mechanism in high voltage diode with the FLR termination structure during reverse recovery by electrothermal simulation. It shows that the high electric field punches through to the termination surface, and a positive feedback process that the physical effects including current filament, high electric field, and high impact ionization influence mutually by themselves at the termination surface, triggering a high temperature by local heating at the center of the carrier-generating located in high-field region, which may lead to the diode destruction at the edge of the termination. Nevertheless, with the decrease of the total current density, the current filament at the edge of the termination disappears, resulting in the

decreased temperature, which should be a self-stabilizing mechanism. Finally, the single current filament essentially driven by thermal mechanism can lead to a dramatic increase in temperature and may cause the destruction by local melting in the active region.

Acknowledgments

This work was supported by National Natural Science Foundation of China [grant number 51477137]; Doctoral Dissertation Innovation Fund of Xi'an University of Technology [grant number 310-252071708]; Specialized Research Fund for the Doctoral Program of Higher Education of China [grant number 20136118110004]; and Industrial Research Project of Science Technology Department Shaanxi Province (grant number 2014K06-21).

References

- [1] J. Q. Xie, *et al.*: "A snapback-free reverse conducting IGBT with recess and floating buffer at the backside," *IEICE Electron. Express* **14** (2017) 20170677 (DOI: 10.1587/elex.14.20170677).
- [2] J. Lutz, *et al.*: "The nn^+ junction as the key to improved ruggedness and soft recovery of power diodes," *IEEE Trans. Electron Devices* **56** (2009) 2825 (DOI: 10.1109/TED.2009.2031019).
- [3] M. Domeij, *et al.*: "Dynamic avalanche in Si power diodes and impact ionization at the nn^+ junction," *Solid-State Electron.* **44** (2000) 477 (DOI: 10.1016/S0038-1101(99)00261-0).
- [4] M. Domeij, *et al.*: "Stable and unstable dynamic avalanche in fast silicon power diodes," *ESSDERC* (2001) 263 (DOI: 10.1109/ESSDERC.2001.195251).
- [5] J. Oetjen, *et al.*: "Current filamentation in bipolar power devices during dynamic avalanche breakdown," *Solid-State Electron.* **44** (2000) 117 (DOI: 10.1016/S0038-1101(99)00209-9).
- [6] L. Zhang and C. Wang: "Influence of carrier lifetime distribution on the current filament in high voltage diode," *Microelectron. Reliab.* **72** (2017) 75 (DOI: 10.1016/j.microrel.2017.04.001).
- [7] J. Lutz and R. Baburske: "Dynamic avalanche in bipolar power devices," *Microelectron. Reliab.* **52** (2012) 475 (DOI: 10.1016/j.microrel.2011.10.018).
- [8] K. Nakamura, *et al.*: "Advanced RFC technology with new cathode structure of field limiting rings for high voltage planar diode," *ISPSD* (2010) 133.
- [9] H.-J. Schulze, *et al.*: "Filament-induced thermomigration of an aluminum drop at the cathode-side of high-voltage power diodes," *ISPSD* (2011) 104 (DOI: 10.1109/ISPSD.2011.5890801).
- [10] X. Cheng, *et al.*: "A general design methodology for the optimal multiple-field-limiting-ring structure using device simulator," *IEEE Trans. Electron Devices* **50** (2003) 2273 (DOI: 10.1109/TED.2003.815132).
- [11] L. Zhang and C. Wang: "A field limiting ring termination structure with a p type corrugated resistance region," *IPEMC* (2016) 1623 (DOI: 10.1109/IPEMC.2016.7512536).
- [12] J. V. Subhas Chandra Bose, *et al.*: "A novel metal field plate edge termination for power devices," *Microelectronics J.* **32** (2001) 323 (DOI: 10.1016/S0026-2692(01)00004-0).
- [13] M.-W. Ha, *et al.*: "The novel junction termination method employing shallow trench," *Phys. Scr.* **2004** (2004) 120 (DOI: 10.1088/0031-8949/2004/T114/030).
- [14] J. Lutz and M. Domeij: "Dynamic avalanche and reliability of high voltage diodes," *Microelectron. Reliab.* **43** (2003) 529 (DOI: 10.1016/S0026-2714(03)00020-9).
- [15] A. Nishii, *et al.*: "Relaxation of current filament due to RFC technology and ballast resistor for robust FWD operation," *ISPSD* (2011) 96 (DOI: 10.1109/ISPSD.2011.5890799).
- [16] F. Masuoka, *et al.*: "Great impact of RFC technology on fast recovery diode towards 600 V for low loss and high dynamic ruggedness," *ISPSD* (2012) 373 (DOI: 10.1109/ISPSD.2012.6229099).

- [17] J. Lutz, *et al.*: *Semiconductor Power Devices: Physics, Characteristics, Reliability* (Springer, Berlin, 2011) 426.
- [18] H. Schulze, *et al.*: “Limiting factors of the safe operating region for power devices,” *IEEE Trans. Electron Devices* **60** (2013) 551 (DOI: [10.1109/TED.2012.2225148](https://doi.org/10.1109/TED.2012.2225148)).
- [19] S. Milady, *et al.*: “Different types of avalanche-induced moving current filaments under the influence of doping inhomogeneities,” *Microelectronics J.* **39** (2008) 857 (DOI: [10.1016/j.mejo.2007.11.004](https://doi.org/10.1016/j.mejo.2007.11.004)).
- [20] B. Heinze, *et al.*: “Ruggedness analysis of 3.3 kV high voltage diodes considering various buffer structures and edge terminations,” *Microelectronics J.* **39** (2008) 868 (DOI: [10.1016/j.mejo.2007.11.023](https://doi.org/10.1016/j.mejo.2007.11.023)).
- [21] C. Wang, *et al.*: “Inhibition of peak electric field shifting on current filaments of high voltage diode,” submitted to *Microelectron. Reliab.*
- [22] C. Wang and L. Zhang: “An analysis of the dynamic avalanche mechanism of an improved FCE diode with a deep p⁺ adjusting region,” *J. Semicond.* **36** (2015) 044006 (DOI: [10.1088/1674-4926/36/4/044006](https://doi.org/10.1088/1674-4926/36/4/044006)).
- [23] J. Lutz: “Fast recovery diodes - reverse recovery behaviour and dynamic avalanche,” *ICM* (2004) 11 (DOI: [10.1109/ICMEL.2004.1314549](https://doi.org/10.1109/ICMEL.2004.1314549)).
- [24] C. Wang and L. Zhang: “Peak electric field shifting induced by avalanche injection under static avalanche in high voltage diode,” *IEICE Electron. Express* **14** (2017) 20170627 (DOI: [10.1587/elex.14.20170627](https://doi.org/10.1587/elex.14.20170627)).
- [25] R. Baburske, *et al.*: “Destruction behavior of power diodes beyond the SOA limit,” *ISPSD* (2012) 365 (DOI: [10.1109/ISPSD.2012.6229097](https://doi.org/10.1109/ISPSD.2012.6229097)).
- [26] R. Baburske, *et al.*: “Cathode-side current filaments in high-voltage power diodes beyond the SOA limit,” *IEEE Trans. Electron Devices* **60** (2013) 2308 (DOI: [10.1109/TED.2013.2264839](https://doi.org/10.1109/TED.2013.2264839)).
- [27] H. P. Felsl, *et al.*: “The CIBH diode - great improvement for ruggedness and softness of high voltage diodes,” *ISPSD* (2008) 173 (DOI: [10.1109/ISPSD.2008.4538926](https://doi.org/10.1109/ISPSD.2008.4538926)).
- [28] H. Egawa: “Avalanche characteristics and failure mechanism of high voltage diodes,” *IEEE Trans. Electron Devices* **ED-13** (1966) 754 (DOI: [10.1109/T-ED.1966.15838](https://doi.org/10.1109/T-ED.1966.15838)).
- [29] B. Heinze, *et al.*: “Ruggedness of high voltage diodes under very hard commutation conditons,” *EPE* (2007) 1 (DOI: [10.1109/EPE.2007.4417776](https://doi.org/10.1109/EPE.2007.4417776)).
- [30] B. K. Boksteen, *et al.*: “6.5 kV field shielded anode (FSA) diode concept with 150 C maximum operational temperature capability,” *ISPSD* (2018) 28 (DOI: [10.1109/ispsd.2018.8393594](https://doi.org/10.1109/ispsd.2018.8393594)).